



## Molecular modeling study on potent and selective adenosine A<sub>3</sub> receptor agonists

Diego Dal Ben, Michela Buccioni, Catia Lambertucci, Gabriella Marucci, Ajiroghene Thomas, Rosaria Volpini, Gloria Cristalli\*

School of Pharmacy, Medicinal Chemistry Unit, University of Camerino, Via S. Agostino 1, 62032 Camerino (MC), Italy

### ARTICLE INFO

#### Article history:

Received 5 May 2010

Revised 9 September 2010

Accepted 16 September 2010

Available online 22 September 2010

#### Keywords:

Adenosine A<sub>3</sub> receptors

Agonist

G protein-coupled receptors

Homology modeling

Molecular docking

### ABSTRACT

Adenosine A<sub>3</sub> receptor (A<sub>3</sub>AR) is involved in a variety of key physio-pathological processes and its agonists are potential therapeutic agents for the treatment of rheumatoid arthritis, dry eye disorders, asthma, as anti-inflammatory agents, and in cancer therapy. Recently reported MECA (5'-N-methylcarboxamidoadenosine) derivatives bearing a methyl group in N<sup>6</sup>-position and an arylolethynyl substituent in 2-position demonstrated to possess sub-nanomolar affinity and remarkable selectivity for the human A<sub>3</sub>AR, behaving as full agonists of this receptor. In this study, we made an attempt to get a rationalization of the high affinities and selectivities of these molecules for the human A<sub>3</sub>AR, by using adenosine receptor (AR) structural models based on the A<sub>2A</sub>AR crystal structure and molecular docking analysis. Post-docking analysis allowed to evaluate the ability of modeling tools in predicting A<sub>3</sub>AR affinity and in providing interpretation of compound substituents effect on the A<sub>3</sub>AR affinity and selectivity.

© 2010 Elsevier Ltd. All rights reserved.

### 1. Introduction

Adenosine (Ado, Fig. 1) modulates a variety of physiological and patho-physiological processes through the activation of at least four G protein-coupled receptors (P1), which have been cloned<sup>1</sup> and classified<sup>2</sup> as adenosine A<sub>1</sub>, A<sub>2A</sub>, A<sub>2B</sub>, and A<sub>3</sub> receptors (A<sub>1</sub>AR, A<sub>2A</sub>AR, A<sub>2B</sub>AR, and A<sub>3</sub>AR, respectively) on the bases of their respective coupling to second messengers, tissue distribution, and unique pharmacological profiles.<sup>2,3</sup> A<sub>3</sub>AR is expressed in a broad range of tissues and its activation leads to inhibition of adenylyl cyclase, raise of intracellular Ca<sup>2+</sup> concentration, and activation of phosphoinositide 3-kinase.<sup>4</sup> It is involved in a variety of key physiological processes such as release of inflammatory mediators and inhibition of tumor necrosis factor- $\alpha$  production.<sup>5–7</sup> Activation of this receptor is suggested to take part in immunosuppression<sup>8</sup> and in the protection from brain and heart ischemia.<sup>9–12</sup> Recent studies suggest that A<sub>3</sub>AR agonists could be employed as therapeutic agents for the treatment of rheumatoid arthritis,<sup>13,14</sup> dry eye disorders,<sup>15</sup> asthma,<sup>16</sup> as anti-inflammatory agents, and in cancer therapy as cytostatic and chemoprotective compounds.<sup>17–19</sup> Hence, the design and synthesis of potent and selective A<sub>3</sub>AR agonists could help to provide tools for further characterization of the physio-pathological roles of this receptor and for the development of new drugs.

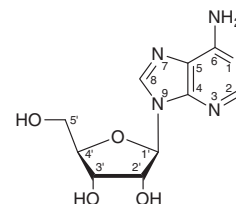


Figure 1. Chemical structure of Ado and atoms numbering.

Previous works tested the ability of Ado derivatives to bind and activate the human A<sub>3</sub>AR, in particular after introduction of (ar)alkynyl chains in 2-position (i.e., 2-phenylethynylAdo or PEAdo) or a methoxy group in N<sup>6</sup>-position of Ado. Further studies evaluated analog modifications applied to 5'-N-methylcarboxamidoAdo (MECA) derivatives. The results showed that both 2- or N<sup>6</sup>-substituted derivatives have higher affinity and in some cases some selectivity for the human A<sub>3</sub>AR than the unmodified nucleosides.<sup>20–23</sup> Functional studies reported in the same works also proved the A<sub>3</sub>AR agonist profile of these compounds. The observation that the introduction of a methyl group in N<sup>6</sup>-position of 2-phenylethynylAdo favors the interaction with the human A<sub>3</sub>AR and the selectivity versus the other AR subtypes<sup>24</sup> led our group to synthesize and evaluate MECA derivatives bearing (ar)alkynyl chains in 2-position and a methyl group in N<sup>6</sup>-position. These compounds proved to possess sub-nanomolar A<sub>3</sub>AR affinity and a remarkable selectivity for this AR subtype, resulting to be among the most potent and selective A<sub>3</sub>AR ligands reported so far.<sup>25</sup>

\* Corresponding author. Tel.: +39 0737 402252; fax: +39 0737 402295.

E-mail addresses: [gloria.cristalli@unicam.it](mailto:gloria.cristalli@unicam.it), [cristall@camserv.unicam.it](mailto:cristall@camserv.unicam.it) (G. Cristalli).

We decided to analyze the particular pharmacological behavior of these molecules by using molecular modeling approaches. In particular, we made an attempt to get a rationalization of the high affinities and selectivities of the presented molecules for the human A<sub>3</sub>AR, by using the recently solved human A<sub>2A</sub>AR crystal structure<sup>26</sup> as template for homology modeling studies and by carrying out docking experiments at the A<sub>1</sub>, A<sub>2A</sub>, and A<sub>3</sub> ARs binding sites. A<sub>2B</sub>AR was not considered in this study as the compounds resulted totally inactive at this AR subtype ( $K_i$  values >30  $\mu$ M).

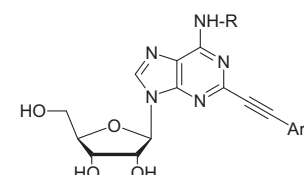
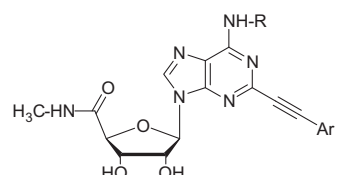
The compounds selected for this analysis were the above cited 2-(ar)alkynyl-N<sup>6</sup>-methyl-MECA derivatives and the analog N<sup>6</sup>-methoxy substituted compounds. We also considered PEAdo and its N<sup>6</sup>-methyl, N<sup>6</sup>-methoxy, and 4'-methylcarboxamido (PEMECA) substituted analogs to evaluate the role of the different substituents of Ado moiety. The list of analyzed compounds is reported in Table 1.

## 2. Results and discussion

### 2.1. Homology modeling and binding site refinement

To rebuild the structural models of human A<sub>1</sub> and A<sub>3</sub> ARs we employed the recently reported crystal structure of human A<sub>2A</sub>AR as 3D template. Considering this structure, experimental evidence suggests that engineering (aimed at increasing the protein stability for the crystallization) may have moved the receptor conformation toward the activated state. This data is indicated by a significantly increased agonist affinity as compared to the wild-type receptor while the antagonist  $K_i$  values are at wild-type A<sub>2A</sub>AR level.<sup>26,27</sup> This is an interesting data indicating the A<sub>2A</sub>AR crystal structure as suitable for modeling studies aimed at simulating receptor-agonist binding interaction. In this sense, a proof is the docking study reported by Ivanov et al.<sup>28</sup> in which the natural agonist Ado was docked into the A<sub>2A</sub>AR crystal structure binding site with no need to significantly alter the residues side chain orientation. The comparative analysis of Ado agonist and ZM241385 antagonist binding mode reported in this work described the agonist adenine ring and the antagonist aromatic system as accommodated in the same region within the putative binding site of the receptor, with the role of agonist ribose moiety in providing additional interaction features in the depth of the binding cavity.

**Table 1**  
Analyzed compounds with corresponding binding affinity data ( $K_i$ , nM values) at human A<sub>1</sub>AR, A<sub>2A</sub>AR, and A<sub>3</sub>AR as reported in literature

			
1	R = H	4	R = H
2	R = OCH <sub>3</sub>	5-8	R = OCH <sub>3</sub>
3	R = CH <sub>3</sub>	9-12	R = CH <sub>3</sub>

Compd	Ar	$K_i$ A <sub>1</sub> AR	$K_i$ A <sub>2A</sub> AR	$K_i$ A <sub>3</sub> AR
1 (PEAdo) <sup>20</sup>	Ph	391	363	16
2 <sup>23</sup>	Ph	1210	4290	3.8
3 <sup>24</sup>	Ph	1690	8530	3.4
4 (PEMECA) <sup>24</sup>	Ph	3920	1760	7.3
5 <sup>23</sup>	Ph	9140	16,300	1.9
6 <sup>23</sup>	<i>p</i> -CH <sub>3</sub> -CO-Ph	53,800	10,400	2.5
7 <sup>23</sup>	<i>p</i> -F-Ph	3000	18,700	1.9
8 <sup>23</sup>	2-Py	3990	18,000	1.1
9 <sup>25</sup>	Ph	32,800	41,700	0.44
10 <sup>25</sup>	<i>p</i> -CH <sub>3</sub> -CO-Ph	10,200	7030	0.33
11 <sup>25</sup>	<i>p</i> -F-Ph	5310	12,700	0.43
12 <sup>25</sup>	2-Py	8740	24,300	0.4

A second important feature of A<sub>2A</sub>AR crystal structure is that it allows to improve the accuracy of AR homology models, due to the high residue conservation in the primary sequences of the AR subtypes, which share a sequence identity of ~57% within the transmembrane (TM) domains.<sup>29</sup> The conservation is higher between A<sub>2A</sub>AR and A<sub>2B</sub>AR, which share a sequence identity of ~70%. Considering overall sequence identity at the amino acid level, the human A<sub>2A</sub>AR shares ~49% amino acid sequence identity with human A<sub>1</sub>AR, ~58% with human A<sub>2B</sub>AR subtype, and ~41% with the human A<sub>3</sub>AR. The residues located within the seven TM domains in the upper part of ARs are highly conserved, with an average identity of 71%.<sup>30</sup> As these residues are involved in interaction with ligand, sequence analysis suggests a common mechanism for ligand recognition for the four subtypes. Despite the high conservation of these regions, specific variable amino acids give unique pharmacological features to the various subtypes and are at the base of different affinities of ligands towards the ARs. A sequence alignment of human ARs is presented in Figure 2.

Our AR modeling approach started from a preliminary manual docking analysis of Ado within the A<sub>2A</sub>AR crystal structure binding site followed by energy minimization.

The localization and orientation of the co-crystallized A<sub>2A</sub>AR antagonist ZM241385 helped in establishing the binding pocket for the preliminary Ado docking analysis. Co-crystallized water molecules were removed before manual docking analysis. Ado binding mode resulted comparable with the one reported by Ivanov et al. (see above) and it is showed in Figure 3. The A<sub>2A</sub>AR-Ado complex was then used as template to homology build models of human A<sub>1</sub> and A<sub>3</sub> ARs. Each AR model in complex with Ado was then refined with energy minimization and subjected to Monte Carlo analysis to explore the favorable binding conformations. The input structure consisted of the ligand and a shell of receptor amino acids within 6 Å distance from the ligand. A second external shell of all the residues within a distance of 8 Å from the first shell was kept fixed. During the Monte Carlo conformational searching, the input structure was modified by random changes in torsion angles (for all input structure residues), and molecular position (for the ligand). Hence, the ligand was left free to be continuously re-oriented and re-positioned within the binding site and the conformation of both ligand and internal shell residues could be explored and reciprocally relaxed. Best receptor-Ado complex for each subtype was energy minimized and saved. After removal of Ado ligand, the final receptor structures were then used for docking analysis of the analyzed compounds.

### 2.2. Molecular docking analysis

All ligand structures were optimized using RHF/AM1 semiempirical calculations and the software package MOPAC implemented in MOE was utilized for these calculations.<sup>31</sup> The compounds were then docked into the binding site of the three AR models by using the MOE Dock tool. Poses generated by the placement methodology were scored using two available methods implemented in MOE, the *London dG* scoring function which estimates the free energy of binding of the ligand from a given pose, and *Affinity dG* Scoring which estimates the enthalpic contribution to the free energy of binding. Top docking pose of each compound was then subjected to MMFF94<sup>32–38</sup> energy minimization. Receptor residues within 6 Å distance from the ligand were left free to move, while the remaining receptor co-ordinates were kept fixed.

The docking conformations share a common motif, presenting the Ado/MECA derivatives located in the binding site with an *anti* conformation (six member ring of adenine and 4'-function of ribose being oppositely oriented). This conformation is in accordance with previously reported studies indicating the inability of Ado analogs restricted to the *syn* conformation to activate ARs.<sup>39–41</sup> Adenine

		TM1		IL1		TM2				
A <sub>1</sub> AR	1	MP---PSISAFQAAAYIGIEVLIALVSVPGNVLVIWAVKVNQALRDATFCFIVSLAVADVA								57
A <sub>2A</sub> AR	1	MP-----I-MGSSVYITVELAIAVLAILGNVLVCWAVWLNLSNLQNVNTNYFVVS�AAADIA								54
A <sub>2B</sub> AR	1	ML-----LETQDALYVALELVIAALSVAGNVLVCAAVGTANTLQTPNTNYFLVSLAAADVA								55
A <sub>3</sub> AR	1	MPNNSTALSLANVTYITMEIFIGLCAIVGNVLVICVVKLNPSLQTTTFYFIVSLALADIA								60
		*		*****		*		* * * * *		
		TM2		EL1		TM3		IL2		
A <sub>1</sub> AR	58	VGALVIPLAILINIGPQTYFHT		CLMVACFV		LILTQSSILALLAIAVDRLRVKI		PLRYKM		117
A <sub>2A</sub> AR	55	VGVLAIPFAITISTGFC		CAACHGCLFIACFV		LVLVTQSSIFSLAIAIDRYIAIRI		PLRYNG		114
A <sub>2B</sub> AR	56	VGLFAIPFAITISLGECTDFYGC		FLFACFV		LVLVTQSSIFSLAVAVDRYLAI		CVPLRYKS		115
A <sub>3</sub> AR	61	VGVLMPLAIVVSLGITIH		FYSCLFMTCCL		LIFTHASIMSLAIAVDRLRVKL		TVRYKR		120
		**		* * *		* 1 2 3 *		* * * * *		**
		IL2		TM4		EL2				
A <sub>1</sub> AR	118	VVTPRRAAVAIAIGCWILSFVVGLTPMFGWNNLSAVERAWAAN--GSMGEP--VIK		EEFEK						173
A <sub>2A</sub> AR	115	LVTGTRAKGIIAICWVLSFAIGLTPMLGWNNGGQPKGKNHS--QGCGEG--QVAC		LFED						170
A <sub>2B</sub> AR	116	LVTGTRARGVIAVLWVLAFIGLTPFLGWNSSKDSATNNCTEPWDGTTNESCCLVK		LFEN						175
A <sub>3</sub> AR	121	VTTHRIWLALGLCWLVSFLVGLTPMFGWNNMMLTSEYHRNVT-----FLSCQFVS								170
		*		*		*****		2		1 3 *
		EL2		TM5		IL3		TM6		
A <sub>1</sub> AR	174	VISMEYMVYFNFFVWVLP		LLLLMLVI		LYLEVLYLIRKQLNKKSAS--SGDPQKY		YGKELK		231
A <sub>2A</sub> AR	171	VVPMMYMVYFNFFACVLV		PLLLMLGV		YLRIFLAARRQLKQMESQPLPGERARST		LQKEVH		230
A <sub>2B</sub> AR	176	VVPMSYMVYFNFFGCVLP		PLLLIMLV		IYIKI FLVACRQLQRTLM---DHSRTTLQREIH				231
A <sub>3</sub> AR	171	VMRMDYMVYFSFLTWFIF		PLVVMCAI		YLDIFYIIRNKLSLNLN---SKETGAF		YGREFK		227
		* * * * *		**		*		*		
		TM6		EL3		TM7				
A <sub>1</sub> AR	232	IAKSLALILFLFALSWLPL		STINCITLFCPSC--HKPSILTYIAIFLTHGNSAMNP		IVYA				289
A <sub>2A</sub> AR	231	AAKSLAIIIVGLFALCWLE		PLHTINCETFFCPCDCS-HAPLWLMYLAIVLSHTNSV		VNFFIYA				289
A <sub>2B</sub> AR	232	AAKSLAMIVGIFALCWLE		VHAVNCVTLFQPAQGNKPKWAMMAILLSHANSV		VNPIVYA				291
A <sub>3</sub> AR	228	TAKSLFLVLFLFALSWLPL		STINCITLYFNGE----		VPQLVLYMGMAILLSHANSMMNP		IVYA		283
		****		*** **		**		4 4 *		* * * * *
		TM7		C-TERM						
A <sub>1</sub> AR	290	FRIQKFRVTEFLKIWNDFRCQPAPPIDEDLPEERPDD-----								326
A <sub>2A</sub> AR	290	YRIREFRQTFRKIIIRSHVLRRQQEPFKAGTSARVLAAGHSDGE								332
A <sub>2B</sub> AR	292	YRNRDFRYTFHKIISRYLLCQADVKSNGGQAGVQPAL-GV-GL								332
A <sub>3</sub> AR	284	YKIKKFKEYTLLILKACVVCHPSDSLDTSEKNS-----								318
		* * *								

**Figure 2.** Sequence alignment of the four human AR subtypes. Transmembrane (TM), intracellular loop (IL), extracellular loop (EL), and C-terminal (C-TERM) domains are indicated; Symbols indicate sequence identity in all the four subtypes; C letters indicate cysteine residues involved in disulfide bridges as observed in A<sub>2A</sub>AR crystal structure and cysteine residues in the other ARs when conserved in all the four subtypes; 1 numbers indicate the cysteine pairs involved in the four disulfide bridges as observed in A<sub>2A</sub>AR crystal structure. R letters indicate non-conserved residues in ligand proximity.

scaffold is positioned between TM3, TM6, and TM7, with the 8- and 9-positions pointing towards the core of the receptor. The 2- and N<sup>6</sup>-substituents are externally located (Fig. 4). The adenine plane is placed in rough correspondence with the ZM241385 antagonist one, with a  $\pi$ -stacking interaction with the conserved Phenylalanine residue (Phe171 in A<sub>1</sub>AR, Phe 168 in A<sub>2A</sub>, and A<sub>3</sub> ARs). The phenylethynyl group in 2-position is located between TM2 and TM7, with the phenyl ring position not corresponding to the one occupied by the analog group of ZM241385 compound. The role played by 2-substituents in interaction with AR is not totally clear. As previously reported, while the presence of an alkylalkynyl group in 2-position provides high affinity for A<sub>1</sub>, A<sub>2A</sub>, and A<sub>3</sub> ARs, the introduction of an arylalkynyl group demonstrates to increase A<sub>3</sub>AR affinity and selectivity.<sup>24</sup> Our modeling studies did not highlight significant interactions between the 2-arylalkynyl substituents and the receptor residues. On the other hand, affinity data show that the presence of substituents on this side group does not significantly modify the  $K_i$  value, suggesting a possible different explanation than a simple hydrophilic or hydrophobic ligand-target contact. Considering the AR structural features around the agonist 2-substituent, it can be noted that A<sub>3</sub>AR contains a smaller EL2 segment respect to A<sub>1</sub>AR and in particular A<sub>2A</sub>AR. The smaller size of this loop in A<sub>3</sub>AR could possibly make larger the binding region of this subtype, allowing the presence of ligands with either flexible or rigid chains in 2-position. On the contrary, in the case of A<sub>1</sub> and A<sub>2A</sub> ARs the steric

hindrance of EL2 could permit the presence of only flexible chains in position 2. This data could explain the effect of 2-arylalkynyl substituent insertion on the ARs affinity, but it obviously needs further investigation.

The compounds ribose moiety is located in depth into the transmembrane helices bundle, in a region between TM2, TM3, TM6, and TM7 in close proximity to a conserved Tryptophan (Trp247 in A<sub>1</sub>AR, Trp246 in A<sub>2A</sub>AR, and Trp243 in A<sub>3</sub>AR) sidechain. The role of this residue has been analyzed in several published studies,<sup>42,43</sup> which proposed its conformational change as one of the possible steps of receptor activation. In our study, the sidechain of the conserved Tryptophan did not considerably change its orientation during Monte Carlo analysis with Ado ligand. The conformational change of this residue (with a reorientation towards the external of the receptor) was more significant during docking poses minimization of MECA derivatives, possibly due to the greater hindrance of substituted 5' group. The ribose ring presents a North-conformation, with the hydroxy group in 3'-position giving H-bond interaction with A<sub>1</sub>AR His278, A<sub>2A</sub>AR Ser277 and His278, and A<sub>3</sub>AR Ser271 and His272 sidechains (Figs. 4 and 5). The 4'-methylcarboxamido substituent of MECA derivatives is located between TM3 and TM6, giving H-bond interaction with A<sub>1</sub>AR Thr91, A<sub>2A</sub>AR Thr88 and Ser277, and A<sub>3</sub>AR Thr94 and Ser271. In the case of Ado derivatives, 4'-position is taken by an hydroxymethyl group able to give H-bond interaction only with A<sub>1</sub>AR Thr91, A<sub>2A</sub>AR Thr88, and A<sub>3</sub>AR Thr94.

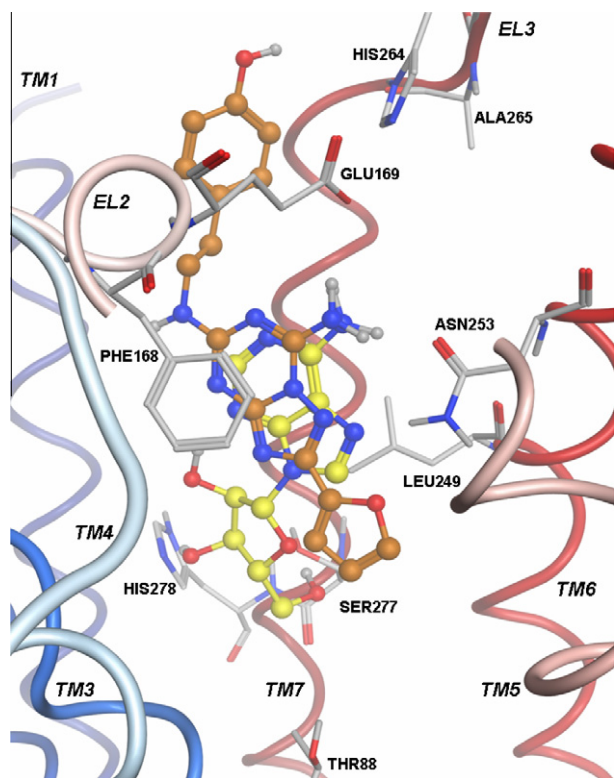


**Figure 3.** Superimposition and comparison of Ado binding mode respect to ZM241385 interaction with A<sub>2A</sub>AR crystal structure. Main residues providing hydrophilic and hydrophobic interaction with ligands are displayed. EL2-TM5 ribbon representation is partially hidden.

The N<sup>6</sup>-amino group and the N-7 atom interact through H-bonding with the conserved Asparagine residue (Asn254 in AA<sub>1</sub>R, Asn253 in AA<sub>2A</sub>R, and Asn250 in AA<sub>3</sub>R), analogously to ZM241385. The N<sup>6</sup>-methyl substituent is located in a sub-pocket that presents different chemical–physical properties in the three analyzed receptor subtypes (Fig. 4). In particular, in the case of A<sub>3</sub>AR this sub-pocket is built by Val169, Ile253, Val259, and Leu264. The corresponding regions in the other subtypes present marked hydrophilic properties, as the A<sub>3</sub>AR Val169 is substituted in the other subtypes by a Glutamate residue, A<sub>3</sub>AR Ile253 by a Threonine, A<sub>3</sub>AR Val259 by a Lysine in A<sub>1</sub>AR and an Alanine in A<sub>2A</sub>AR, and A<sub>3</sub>AR Leu264 by a Threonine in the case of A<sub>1</sub>AR and a Methionine in the case of A<sub>2A</sub>AR.

The docking poses highlight these differences in ligand–receptor contact, as in the case of A<sub>1</sub> and A<sub>2A</sub> ARs the derivatives with unsubstituted amino group in 6-position interact with the receptor through an additional H-bond with a Glutamate residue (Glu172 and Glu169, respectively). The presence of a methyl group as substituent of one of the hydrogen atoms of N<sup>6</sup>-amine prevents this group from giving this interaction. On the other hand, the methyl group in N<sup>6</sup>-position results better accommodated in the hydrophobic sub-pocket of A<sub>3</sub>AR. This data was further analyzed for the interpretation of the higher A<sub>3</sub>AR affinity and selectivity of N<sup>6</sup>-methyl derivatives respect to the corresponding N<sup>6</sup>-unsubstituted compounds (see below).

### 2.3. Post-docking analysis

Top docking pose at A<sub>3</sub>AR of each compound was rescored using the *scoring.svl* script retrievable at the SVL exchange service (Chemical Computing Group, Inc. SVL exchange: <http://svl.chem-comp.com>). This tool allows estimating the 'dock\_p*K*<sub>i</sub>' value by analyzing H-bonds, transition metal, water bridges, and hydrophobic

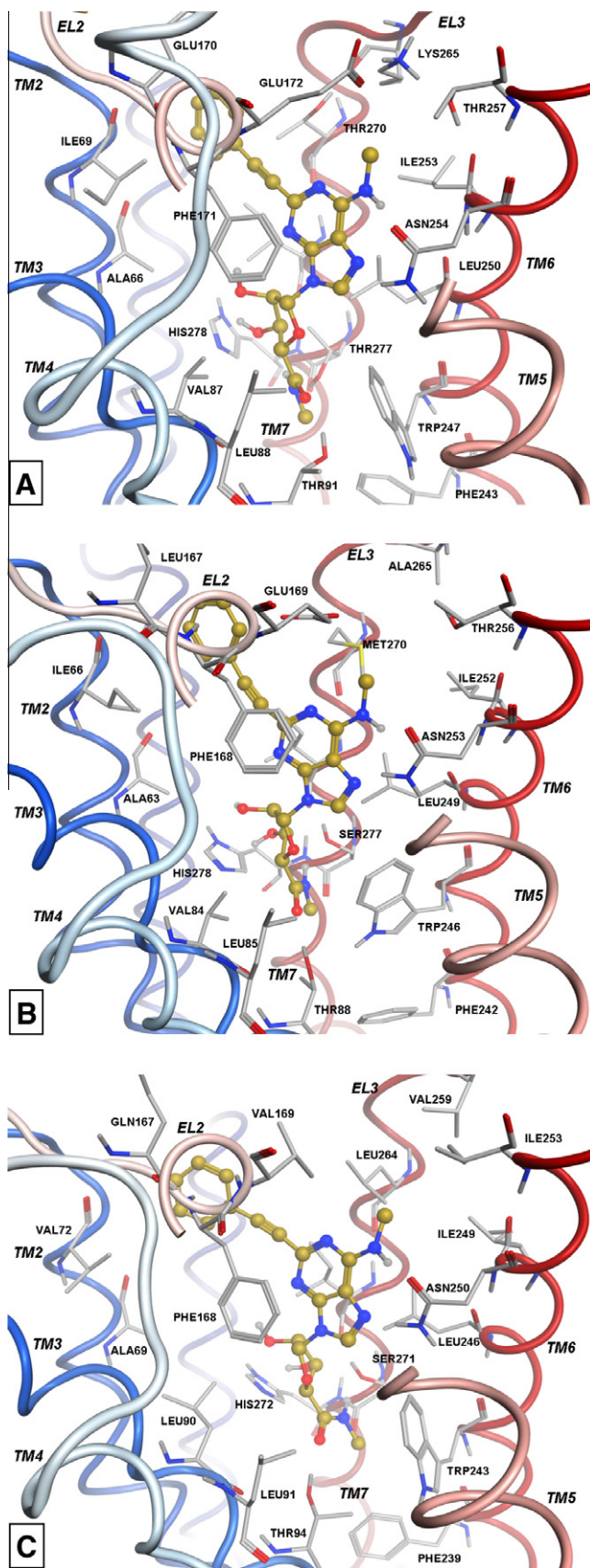


**Figure 4.** Docking pose of compound 9 within A<sub>1</sub>AR (A), A<sub>2A</sub>AR (B), and A<sub>3</sub>AR (C) binding sites. Residues within 4.5 Å distance from ligand are displayed. EL2-TM5 ribbon representation is partially hidden.

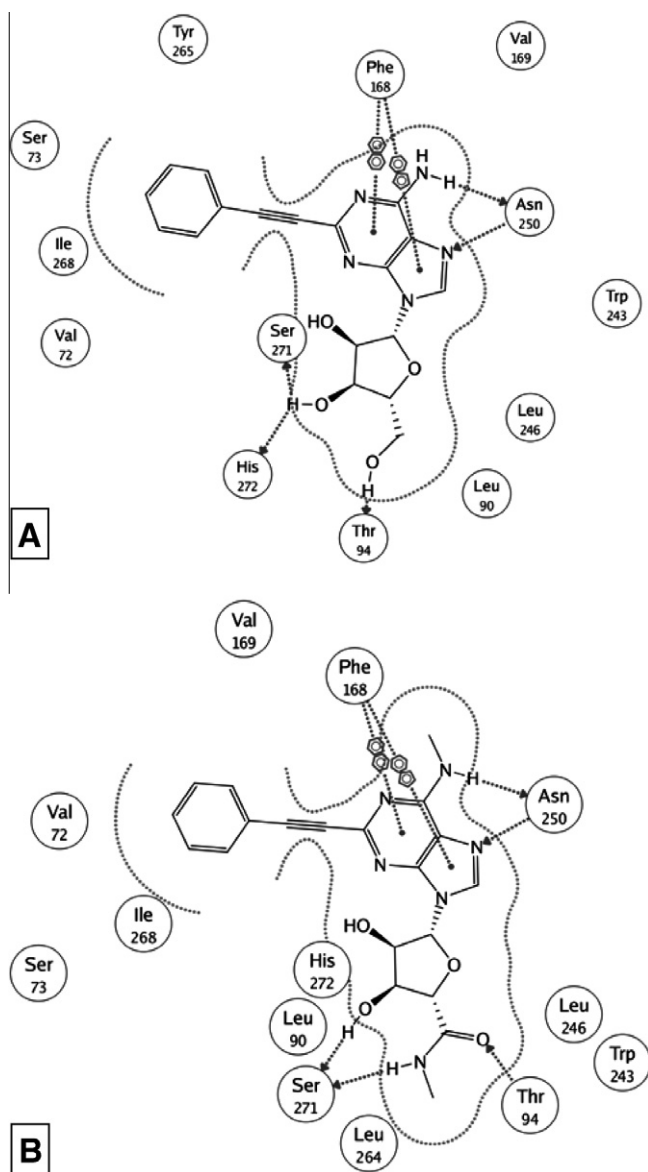


**Figure 5.** Schematic view of compound **1** (A) and **9** (B) interaction with human A<sub>3</sub>AR binding site residues.

intermolecular interactions. The aim of this step was to verify the ability of the script to score the docking poses, giving a compounds ranking in agreement with the experimental affinity values. The script was applied and the obtained values gave a compounds ranking in agreement with experimental pK<sub>i</sub> data trend, with a R<sup>2</sup> value = 0.89. The affinity data were then re-calculated according to the 'exp. pK<sub>i</sub>' – 'dock\_pK<sub>i</sub>' values correlation equation developed within MOE: 'calcd pK<sub>i</sub>' = 4.25 + 1.13 (dock\_pK<sub>i</sub>). The calculated pK<sub>i</sub> values resulted in high agreement with the experimental data, with an average error = 0.16 (data reported in Table 2). It must be underlined that the 'calcd pK<sub>i</sub>' values are docking scores with no physical meaning and are not predictive of binding affinity.

The introduction of 4'-methylcarboxamido and N<sup>6</sup>-methyl substituents on one hand improves the A<sub>3</sub>AR affinity of about 40 fold, on the other hand increases the selectivity versus A<sub>1</sub> and A<sub>2A</sub> ARs of about 85- and 115-fold, respectively, respect to the unsubstituted compound PEAdo (see Table 1). The effect of each substituent is somehow independent from the other one, as it can be depicted by comparing compound **1** and **4** for the role of 4'-substituent and compound **1** and **3** for the role of N<sup>6</sup>-position. On these bases, we performed a

**Table 2**

Comparison of experimental and calculated pK<sub>i</sub> values at A<sub>3</sub>AR for the analyzed compounds

Compd	Exp. pK <sub>i</sub> <sup>a</sup>	Dock_pK <sub>i</sub> <sup>b</sup>	Calcd pK <sub>i</sub> <sup>c</sup>
<b>1</b>	7.80	3.16	7.82
<b>2</b>	8.42	3.45	8.15
<b>3</b>	8.47	3.98	8.75
<b>4</b>	8.14	3.39	8.08
<b>5</b>	8.72	4.14	8.93
<b>6</b>	8.60	4.02	8.79
<b>7</b>	8.72	4.10	8.88
<b>8</b>	8.96	4.22	9.02
<b>9</b>	9.36	4.37	9.19
<b>10</b>	9.48	4.51	9.35
<b>11</b>	9.37	4.35	9.17
<b>12</b>	9.40	4.47	9.30

<sup>a</sup> Experimental pK<sub>i</sub> values at A<sub>3</sub>AR calculated as –log(pK<sub>i</sub>).

<sup>b</sup> Dock\_pK<sub>i</sub> values obtained by applying the MOE scoring.svl script to the best docking conformation at A<sub>3</sub>AR of each compound.

<sup>c</sup> Affinity data re-calculated according to: 'calcd pK<sub>i</sub>' = 4.25 + 1.13 (dock\_pK<sub>i</sub>).

further analysis of the interactions between the compounds and the receptors binding site by using the IF-E 6.0<sup>44</sup> tool retrievable at the SVL exchange service. The script calculates and displays atomic and residue interaction forces as 3D vectors. It also calculates the per-residue interaction energies (values in kcal/mol), where negative and positive energy values are associated to favorable and unfavorable interactions, respectively. This final step was aimed in particular at analyzing the interaction of AR residues with the compound 4'- and N<sup>6</sup>-position and the effect of eventual presence of substituents in the same positions on to the ligand–receptor interaction. The interaction energy differences were considered only from a qualitative point of view and for each AR subtype were considered only some residues located around the compounds N<sup>6</sup>- and 4'-position. At the same time we probed the role of binding site residues that are not conserved among the AR subtypes, to possibly explain the compounds A<sub>3</sub>AR selectivity. For this analysis we considered compound **9** (K<sub>i</sub> A<sub>1</sub>AR = 32,800 nM; K<sub>i</sub> A<sub>2A</sub>AR = 41,700 nM; K<sub>i</sub> A<sub>3</sub>AR = 0.44 nM), which presents a methylcarboxamido and a methyl group in 4'- and N<sup>6</sup>-position, respectively. As comparison term we selected compound **1** (PEAdo, K<sub>i</sub> A<sub>1</sub>AR = 391; K<sub>i</sub> A<sub>2A</sub>AR = 363 nM; K<sub>i</sub> A<sub>3</sub>AR = 16 nM), that is, unsubstituted in these positions. The IF-E 6.0 script was applied to both the A<sub>1</sub>AR-, A<sub>2A</sub>AR-, and A<sub>3</sub>AR-compd **9** and A<sub>1</sub>AR-, A<sub>2A</sub>AR-, and A<sub>3</sub>AR-compd **1** complexes and the interaction energies for each binding site residue within a 10 Å distance from ligand were collected. Table 3 displays the interaction energies for the AR residues in 4'- and in N<sup>6</sup>-substituent proximity, respectively.

The comparative analysis of compounds interaction with A<sub>1</sub>, A<sub>2A</sub>, and A<sub>3</sub> ARs showed that 4'-methylcarboxamido substituent increases the H-bonding ability of the compounds, as already reported during the docking poses description. In fact, the interaction energy with the H-bond counterpart residues is improved from Ado to MECA derivatives considering all three ARs, with a remarkable impact for A<sub>3</sub>AR (A<sub>1</sub>AR: Thr91 + Thr277 + His278 int. energy = –6.10 for compd **1**; –7.68 for compd **9**; A<sub>2A</sub>AR: Thr88 + Ser277 + His278 int. energy = –8.46 for compd **1**; –9.94 for compd **9**; A<sub>3</sub>AR: Thr94 + Ser271 + His272 int. energy = –6.72 for compd **1**; –11.78 for compd **9**). On the other hand, the hydrophobic residues located about the 4'-substituent present an opposite interaction profile respect to the hydrophilic ones, as in general the interaction energy is improved from MECA to Ado derivatives, with a significant interaction energy difference (between compound **1** and **9**) considering A<sub>1</sub> and A<sub>2A</sub> ARs (A<sub>1</sub>AR: Val87 + Leu88 + Trp247 + Leu250 + Ile274 int. energy = –12.13 for compd **1**; –8.81 for compd **9**; A<sub>2A</sub>AR: Val84 + Leu85 + Trp246 + Leu249 + Ile274 int. energy = –16.00 for compd **1**; –7.34 for compd **9**; A<sub>3</sub>AR: Leu90 + Leu91 + Trp243 + Leu246 + Ile268 int. energy = –9.29 for compd **1**; –8.92 for

**Table 3**Ligand–receptor interaction energies (per-residue values) calculated with *IF-E 6.0* script

Substitution	A <sub>1</sub> AR residue	Int. energy		A <sub>2A</sub> AR residue	Int. energy		A <sub>3</sub> AR residue	Int. energy	
		Compd <b>1</b>	Compd <b>9</b>		Compd <b>1</b>	Compd <b>9</b>		Compd <b>1</b>	Compd <b>9</b>
4'-position	Val87	−2.31	−1.35	Val84	−1.76	−0.37	Leu90	−1.12	−0.79
	Leu88	−3.86	−2.18	Leu85	−1.44	−0.75	Leu91	−0.89	−0.63
	Thr91	−3.83	−5.27	Thr88	−0.57	−1.26	Thr94	−3.87	−6.16
	Trp247	−0.57	−2.03	Trp246	−1.88	−0.84	Trp243	−1.86	−2.55
	Leu250	−3.53	−2.02	Leu249	−5.28	−3.01	Leu246	−2.83	−2.47
	His251	−1.83	−0.99	His250	−1.53	0.10	Ser247	−0.01	0.22
	Ile274	−1.86	−1.24	Ile274	−5.65	−2.38	Ile268	−2.59	−2.48
	Thr277	−1.69	−1.35	Ser277	−3.19	−4.60	Ser271	−0.99	−2.78
	His278	−0.58	−1.06	His278	−4.69	−4.08	His272	−1.86	−2.85
	TOT	−20.06	−17.48	TOT	−25.99	−17.18	TOT	−16.02	−20.49
N <sup>6</sup> -position	Phe171	−8.11	−4.43	Phe168	−8.90	−5.74	Phe168	−6.02	−6.30
	Glu172	−10.04	−3.66	Glu169	−9.95	−1.62	Val169	−2.21	−2.94
	Met177	−0.36	−0.41	Met174	−0.12	−0.14	Met174	−0.29	−0.45
	Leu253	−1.49	−1.48	Ile252	−0.71	−0.50	Ile249	−0.31	−0.49
	Asn254	−6.04	−4.57	Asn253	−2.97	−1.90	Asn250	−3.23	−2.92
	Thr257	−0.82	−1.29	Thr256	−0.98	−0.96	Ile253	−0.35	−0.99
	Lys265	−0.63	1.20	Ala265	−0.40	0.11	Val259	−0.45	−0.47
	Thr270	−1.68	−1.51	Met270	−3.38	−4.87	Leu264	−2.71	−2.60
	TOT	−29.16	−16.18	TOT	−27.41	−15.61	TOT	−15.57	−17.16

Data for AR residues located in proximity of 4'- and N<sup>6</sup>-position of compound **1** and **9** are displayed. Data are expressed as kcal/mol.

compd **9**). Among these residues, the A<sub>3</sub>AR Leu90 is not conserved in the other subtypes, as in A<sub>1</sub> and A<sub>2A</sub> ARs its position is taken by a Valine. Interaction energy values of this residue are comparable for compound **1** and **9**, while analog comparison considering A<sub>1</sub>AR Val87 and A<sub>2A</sub>AR Val84 shows a significant difference between interaction energies of the two compounds. As Leucine and Valine present similar chemical–physical properties, this result could be explained considering that the presence of the 4'-substituent could have some steric effect, that is, different among the AR subtypes. Similar trend is noted considering another non-conserved residue, A<sub>3</sub>AR Ser247 (His251 and His250 in A<sub>1</sub> and A<sub>2A</sub> ARs, respectively). The sum of the interaction energy values of hydrophilic and hydrophobic residues leads to a divergent behavior of the AR binding site considering the interaction with 4'-substituent, as in the case of A<sub>1</sub> and A<sub>2A</sub> ARs the interaction seems more favorable with Ado derivative, while the MECA 4'-methylcarboxamido function is preferred by A<sub>3</sub>AR residues respect to the corresponding Ado 4'-hydroxymethyl group (A<sub>1</sub>AR: 'total' int. energy with 4'-substituent = −20.06 for compd **1**; −17.48 for compd **9**; A<sub>2A</sub>AR: 'total' int. energy = −25.99 for compd **1**; −17.18 for compd **9**; A<sub>3</sub>AR: 'total' int. energy = −16.02 for compd **1**; −20.49 for compd **9**). Analog analysis was performed on the AR residues located about the N<sup>6</sup>-group. It must be noted that all the A<sub>3</sub>AR residues located in proximity of this substituent are hydrophobic. An exception is Asn250, that is, conserved among ARs and plays a key role in ligand interaction, as observed even in A<sub>2A</sub>AR–ZM241385 complex crystal structure. This residue presents a similar interaction trend for all the three AR subtypes, with more favorable interaction energy values for N<sup>6</sup>-unsubstituted compounds. This result is more evident for A<sub>1</sub> and A<sub>2A</sub> ARs (A<sub>1</sub>AR: Asn254 int. energy = −6.04 for compd **1**; −4.57 for compd **9**; A<sub>2A</sub>AR: Asn253 int. energy = −2.97 for compd **1**; −1.90 for compd **9**; A<sub>3</sub>AR: Asn250 int. energy = −3.23 for compd **1**; −2.92 for compd **9**). Considering the remaining A<sub>3</sub>AR residues located around N<sup>6</sup>-substituent, in general the interaction energy values present a similar trend indicating a preference for N<sup>6</sup>-methyl substituted derivatives, with the exception of Leu264. The same analysis performed for A<sub>1</sub> and A<sub>2A</sub> ARs presents different results, with a significantly more favorable interaction with N<sup>6</sup>-unsubstituted compounds. As described above, the location of N<sup>6</sup>-group is between the top regions of TM domains and in proximity of EL segments. These sites present several non-conserved residues among ARs, one of which is a Glutamate in A<sub>1</sub>AR (Glu172) and A<sub>2A</sub>AR (Glu169). The A<sub>2A</sub>AR crystal structure puts in evidence the role of this residue in interaction with ZM241385 ligand through

an H-bond between the residue carboxy function and the antagonist free amino group. Analog result is observed for N<sup>6</sup>-unsubstituted compounds in this study.

This residue is substituted in A<sub>3</sub>AR by a Valine (Val169). As consequence, the hydrophobic profile of its side chain on one hand leads to the loss of H-bonding ability, on the other hand can favor the presence of ligand hydrophobic substituents. The comparison of interaction energy for these Glutamate and Valine residues demonstrates the different AR preference for N<sup>6</sup>-unsubstituted (A<sub>1</sub> and A<sub>2A</sub> ARs) or substituted (A<sub>3</sub>AR) compounds (A<sub>1</sub>AR: Glu172 int. energy = −10.04 for compd **1**; −3.66 for compd **9**; A<sub>2A</sub>AR: Glu169 int. energy = −9.95 for compd **1**; −1.62 for compd **9**; A<sub>3</sub>AR: Val169 int. energy = −2.21 for compd **1**; −2.94 for compd **9**). The presence of the substituent seems to affect also the  $\pi$ -stacking interaction with the conserved Phenylalanine residue (Phe171 in A<sub>1</sub>AR, Phe168 in A<sub>2A</sub>AR and A<sub>3</sub>AR), as the interaction of A<sub>1</sub> and A<sub>2A</sub> AR residues appears significantly higher with N<sup>6</sup>-unsubstituted derivatives, while A<sub>3</sub>AR Phe168 presents a comparable interaction with substituted and unsubstituted compounds. Considering the remaining residues around the N<sup>6</sup>-group, in general the hydrophobic residues present different degrees of preference for N<sup>6</sup>-methyl substituted derivatives, while the hydrophilic residues present more favorable interaction with the unsubstituted compounds (with the exception of A<sub>1</sub>AR Thr257). Even in this case, the sum of the interaction energy values of hydrophilic and hydrophobic residues leads to a divergent behavior of the AR binding site considering the interaction with N<sup>6</sup>-substituent. (A<sub>1</sub>AR: 'total' int. energy with N<sup>6</sup>-substituent = −29.16 for compd **1**; −16.18 for compd **9**; A<sub>2A</sub>AR: 'total' int. energy = −27.41 for compd **1**; −15.61 for compd **9**; A<sub>3</sub>AR: 'total' int. energy = −15.57 for compd **1**; −17.16 for compd **9**). Considering a comparison of N<sup>6</sup>-methyl and N<sup>6</sup>-methoxy substituted derivatives, it can be noted that these groups present similar chemical–physical properties and as expected the interaction energies show a similar trend (data not shown). Hence, the average higher affinity of N<sup>6</sup>-methyl substituted compounds respect to the N<sup>6</sup>-methoxy substituted ones could be explained in terms of steric properties, by considering a slight preference of A<sub>3</sub>AR for the smaller substituent.

This analysis suggests that even if the binding mode was conserved among the analyzed molecules, minimal differences in ligand structures or binding site residues could help in explaining the different pharmacological behavior of these compounds at ARs. Even if no direct correlation was made between interaction

energy data and affinity values, it must be noted that the presence of methyl group in N<sup>6</sup>-position and a carboxymethyl function in 4'-position (i.e., the structural differences between compounds **1** and **9**) led to a decrease (absolute values) of interaction energy of about 16 kcal/mol at A<sub>1</sub>AR and 21 kcal/mol at A<sub>2A</sub>AR and an increase of about 6 kcal/mol at A<sub>3</sub>AR, in agreement with the experimental data.

### 3. Conclusion

The recent crystallization of human A<sub>2A</sub>AR is of great impact and utility for the analysis of purinergic receptors structures, for the rationalization of the different binding affinities of their ligands, and for the design of new molecules with improved affinity and selectivity at human ARs. In fact, even if the modeling studies on these receptors carried out by using bovine rhodopsin crystal structure as template provided good indications on agonist- and antagonist–receptor interaction,<sup>23,41</sup> the human A<sub>2A</sub>AR structure allows to get a more accurate depiction of ligand binding modes. In this study we made an attempt to explain the particular pharmacological profile of a set of human A<sub>3</sub>AR agonists presenting the general Ado scaffold with additional substitutions in 2-, N<sup>6</sup>-, and 4'-position. For this analysis we employed AR structural models based on the A<sub>2A</sub>AR crystal structure and optimized with Ado manual docking and Monte Carlo analysis. Each AR model was then used for docking analysis of the analyzed compounds. Post-docking analysis allowed to evaluate the ability of MOE *dock\_pK<sub>i</sub>* scoring function in predicting A<sub>3</sub>AR affinity. Per-residue interaction energy analysis with *IF-E 6.0* script implemented in MOE finally helped to explain the great impact of 4'-methylcarboxamido and N<sup>6</sup>-methyl substituents on the AR affinity and on the A<sub>3</sub>AR selectivity, with an interpretation of the role of AR non-conserved residues.

### 4. Experimental section

All molecular modeling studies were performed on a 2 CPU (PIV 2.0–3.0 GHz) Linux PC. Homology modeling, energy minimization, and docking studies were carried out using Molecular Operating Environment (MOE, version 2008.10) suite.<sup>45</sup> Manual docking and Monte Carlo studies of Ado binding mode were done using Schrodinger Macromodel (ver. 8.0)<sup>46</sup> with Schrodinger Maestro interface. Compounds docking analyzes were then performed with MOE. All ligand structures were optimized using RHF/AM1 semi-empirical calculations and the software package MOPAC implemented in MOE was utilized these calculations.<sup>31</sup>

#### 4.1. Refinement of A<sub>2A</sub>AR structural model

The recently solved X-ray crystal structure of the human A<sub>2A</sub>AR (in complex with ZM241385, pdb code: 3EML;<sup>26</sup> available at the RCSB Protein Data Bank; 2.6 Å resolution) was added of the Pro149-His155 segment (whose structure was not solved by X-ray) and the hydrogen atoms and then subjected to refinement that was AMBER99 energy minimization performed by 1000 steps of steepest descent followed by conjugate gradient minimization until the RMS gradient of the potential energy was <0.05 kJ mol<sup>-1</sup> Å<sup>-1</sup>.

#### 4.2. Preliminary docking analysis with Ado

A preliminary docking analysis was performed by manually docking Ado structure within the A<sub>2A</sub>AR crystal structure binding site. The localization and orientation of the co-crystallized A<sub>2A</sub>AR antagonist ZM241385 helped in establishing the binding pocket for the preliminary Ado docking analysis. The obtained A<sub>2A</sub>AR–Ado complex was then subjected to energy minimization refinement with the same protocol as above.

#### 4.3. Homology modeling of the human A<sub>1</sub> and A<sub>3</sub> ARs

Homology models of the human A<sub>1</sub> and A<sub>3</sub> ARs were built using the A<sub>2A</sub>AR–Ado complex as template. The alignment of the AR primary sequences was built within MOE. For each subtype, template–target alignment was used for the homology modeling protocol, while the boundaries identified from the X-ray crystal structure of human A<sub>2A</sub>AR were applied for the corresponding sequences of each AR subtype. The missing loop domains of the A<sub>1</sub> and A<sub>3</sub> ARs were built by the loop search method implemented in MOE. Once the heavy atoms were modeled, all hydrogen atoms were added, and the protein co-ordinates were then minimized with MOE using the AMBER99 force field.<sup>47</sup> The minimizations were performed by 1000 steps of steepest descent followed by conjugate gradient minimization until the RMS gradient of the potential energy was <0.05 kJ mol<sup>-1</sup> Å<sup>-1</sup>.

#### 4.4. Manual docking: Ado binding mode refinement

The three AR models in complex with Ado were subjected to Monte Carlo analysis to explore the favorable binding conformations. This analysis was conducted by Monte Carlo Conformational Search protocol implemented in Schrodinger Macromodel. The input structure consisted of the ligand and a shell of receptor amino acids within the specified distance (6 Å) from the ligand. A second external shell of all the residues within a distance of 8 Å from the first shell was kept fixed. During the Monte Carlo conformational searching, the input structure was modified by random changes in user-specified torsion angles (for all input structure residues), and molecular position (for the ligand). Hence, the ligand was left free to be continuously re-oriented within the binding site and the conformation of both ligand and internal shell residues could be explored and reciprocally relaxed. The method consisted of 10,000 Conformational Search steps with MMFF94s force field.<sup>32–38</sup> Best receptor–Ado complex for each subtype was saved. The final complexes were input in MOE and subjected to 1000 steps of steepest descent followed by conjugate gradient minimization until the RMS gradient of the potential energy was <0.05 kJ mol<sup>-1</sup> Å<sup>-1</sup>. After removal of Ado ligand, the final receptor structures were used for analyzed compounds docking study.

#### 4.5. Molecular docking analysis

All compound structures were docked into the binding site of the three AR models by using the MOE Dock tool. This method is divided into a number of stages: *Conformational Analysis of ligands*. The algorithm generated conformations from a single 3D conformation by conducting a systematic search. In this way, all combinations of angles were created for each ligand. *Placement*. A collection of poses was generated from the pool of ligand conformations using Alpha Triangle placement method. Poses were generated by superposition of ligand atom triplets and triplets points in the receptor binding site. The receptor site points are alpha sphere centers which represent locations of tight packing. At each iteration a random conformation was selected, a random triplet of ligand atoms and a random triplet of alpha sphere centers were used to determine the pose. *Scoring*. Poses generated by the placement methodology were scored using two available methods implemented in MOE, the *London dG* scoring function which estimates the free energy of binding of the ligand from a given pose, and *Affinity dG* Scoring which estimates the enthalpic contribution to the free energy of binding. Top 30 poses for each ligand were output in a MOE database. Top docking pose at of each compound was then subjected to MMFF94<sup>32–38</sup> energy minimization until the RMS gradient of the potential energy was <0.05 kJ mol<sup>-1</sup> Å<sup>-1</sup>. In this phase, AMBER99 partial charges of receptor and MOPAC

output partial charges of ligands were conserved. Receptor residues within 6 Å distance from the ligand were left free to move, while the remaining receptor co-ordinates were kept fixed.

#### 4.6. Post-docking analysis. Rescoring

For each compound, the minimized top docking pose at A<sub>3</sub>AR was rescored using the *dock-pK<sub>i</sub>* predictor. This tool allows estimating the pK<sub>i</sub> for each ligand using the *scoring.svl* script retrievable at the SVL exchange service (Chemical Computing Group, Inc. SVL exchange: <http://svl.chemcomp.com>) The algorithm is based upon an empirical scoring function consisting of a directional hydrogen-bonding term, a directional hydrophobic interaction term, and an entropic term (ligand rotatable bonds immobilized in binding). Once applied the *dock\_pK<sub>i</sub>* script with default settings, the obtained values were correlated with experimental pK<sub>i</sub> data at A<sub>3</sub>AR and then recalculated according to the 'exp. pK<sub>i</sub>' – 'dock\_pK<sub>i</sub>' values correlation equation: 'calcd pK<sub>i</sub>' = 4.25 + 1.13 (dock\_pK<sub>i</sub>).

#### 4.7. Post-docking analysis. Residue interaction analysis

The interactions between the ligands and the receptors binding site were analyzed by using the *IF-E 6.0* tool retrievable at the SVL exchange service. The program calculates and displays the atomic and residue interaction forces as 3D vectors. It also calculates the per-residue interaction energies, where negative and positive energy values are associated to favorable and unfavorable interactions, respectively. For each AR subtype, a shell of residues contained within a 10 Å distance from ligand were considered for this analysis.

#### Acknowledgments

This work was supported by Fondo di Ricerca di Ateneo (University of Camerino) and Grants from the Italian Ministry for Health (Progetto Ordinario Neurolesi, RF-CNM-2007-662855) and Italian Ministry for University and Research (PRIN2008).

#### References and notes

- Robeva, A. S.; Woodard, R. L.; Jin, X.; Gao, Z.; Bhattacharya, S.; Taylor, H. E.; Rosin, D. L.; Linden, J. *Drug Dev. Res.* **1996**, 39, 243.
- Fredholm, B. B.; Iljerman, A. P.; Jacobson, K. A.; Klotz, K.-N.; Linden, J. *Pharmacol. Rev.* **2001**, 53, 527.
- Cristalli, G.; Volpini, R. *Curr. Top. Med. Chem.* **2003**, 3, 355.
- Englert, M.; Quittner, U.; Klotz, K.-N. *Biochem. Pharmacol.* **2002**, 64, 61.
- Jacobson, K. A.; Gao, Z. G. *Nat. Rev. Drug. Discov.* **2006**, 5, 247.
- Rorke, S.; Holgate, S. T. *Am. J. Respir. Med.* **2002**, 1, 99.
- Jacobson, K. A. *Trends Pharmacol. Sci.* **1998**, 19, 184.
- Baharav, E.; Bar-Yehuda, S.; Madi, L.; Silberman, D.; Rath-Wolfson, L.; Halpren, M.; Ochaion, A.; Weinberger, A.; Fishman, P. *J. Rheumatol.* **2005**, 32, 469.
- Pugliese, A. M.; Coppi, E.; Spalluto, G.; Corradetti, R.; Pedata, F. *Br. J. Pharmacol.* **2006**, 147, 524.
- Headrick, J. P.; Peart, J. *Vasc. Pharmacol.* **2005**, 42, 271.
- Shryock, J. C.; Belardinelli, L. *Am. J. Cardiol.* **1997**, 79, 2.
- Shneyvays, V.; Zinman, T.; Shainberg, A. *Cell Calcium* **2004**, 36, 387.
- Bar-Yehuda, S.; Silverman, M. H.; Kerns, W. D.; Ochaion, A.; Cohen, S.; Fishman, P. *Expert Opin. Investig. Drugs* **2007**, 16, 1601.
- Borea, P. A.; Gessi, S.; Bar-Yehuda, S.; Fishman, P. *Handb. Exp. Pharmacol.* **2009**, 297.
- Fishman, P.; Lorber, I.; Cohn, I.; Reitblat, T. Patent WO2006011130, 2006.
- Meade, C. J.; Dumont, I.; Worrall, L. *Life Sci.* **2001**, 69, 1225.
- Fishman, P.; Bar-Yehuda, S.; Madi, L.; Cohn, I. *Anticancer Drugs* **2002**, 13, 437.
- Madi, L.; Ochaion, A.; Rath-Wolfson, L.; Bar-Yehuda, S.; Erlanger, A.; Ohana, G.; Harish, A.; Merimski, O.; Barer, F.; Fishman, P. *Clin. Cancer Res.* **2004**, 10, 4472.
- Fishman, P.; Bar-Yehuda, S.; Synowitz, M.; Powell, J. D.; Klotz, K.-N.; Gessi, S.; Borea, P. A. *Handb. Exp. Pharmacol.* **2009**, 399.
- Volpini, R.; Costanzi, S.; Lambertucci, C.; Vittori, S.; Cristalli, G. *Curr. Pharm. Des.* **2002**, 8, 2285.
- Cristalli, G.; Camaioni, E.; Costanzi, S.; Vittori, S.; Volpini, R.; Klotz, K.-N. *Drug. Dev. Res.* **1998**, 45, 176.
- Cristalli, G.; Camaioni, E.; Vittori, S.; Volpini, R.; Borea, P. A.; Conti, A.; Dionisotti, S.; Ongini, E.; Monopoli, A. *J. Med. Chem.* **1995**, 38, 1462.
- Volpini, R.; Dal Ben, D.; Lambertucci, C.; Taffi, S.; Vittori, S.; Klotz, K.-N.; Cristalli, G. *J. Med. Chem.* **2007**, 50, 1222.
- Volpini, R.; Costanzi, S.; Lambertucci, C.; Taffi, S.; Vittori, S.; Klotz, K.-N.; Cristalli, G. *J. Med. Chem.* **2002**, 45, 3271.
- Volpini, R.; Buccioni, M.; Dal Ben, D.; Lambertucci, C.; Lammi, C.; Marucci, G.; Ramadori, A. T.; Klotz, K.-N.; Cristalli, G. *J. Med. Chem.* **2009**, 52, 7897.
- Jaakola, V. P.; Griffith, M. T.; Hanson, M. A.; Cherezov, V.; Chien, E. Y.; Lane, J. R.; Iljerman, A. P.; Stevens, R. C. *Science* **2008**, 322, 1211.
- Mustafi, D.; Palczewski, K. *Mol. Pharmacol.* **2009**, 75, 1.
- Ivanov, A. A.; Barak, D.; Jacobson, K. A. *J. Med. Chem.* **2009**, 52, 3284.
- Dal Ben, D.; Lambertucci, C.; Marucci, G.; Volpini, R.; Cristalli, G. *Curr. Top. Med. Chem.* **2010**, 10, 993.
- Costanzi, S.; Ivanov, A. A.; Tikhonova, I. G.; Jacobson, K. A. *Front. Drug Des. Discov.* **2007**, 3, 63.
- Stewart, J. J. *J. Comput. Aided Mol. Des.* **1990**, 4, 1.
- Halgren, T. A. *J. Comput. Chem.* **1996**, 17, 490.
- Halgren, T. A. *J. Comput. Chem.* **1996**, 17, 520.
- Halgren, T. A. *J. Comput. Chem.* **1996**, 17, 553.
- Halgren, T. A. *J. Comput. Chem.* **1996**, 17, 587.
- Halgren, T. A.; Nachbar, R. *J. Comput. Chem.* **1996**, 17, 616.
- Halgren, T. A. *J. Comput. Chem.* **1999**, 20, 720.
- Halgren, T. A. *J. Comput. Chem.* **1999**, 20, 730.
- Bruns, R. F. *Can. J. Physiol. Pharmacol.* **1980**, 58, 673.
- Cristalli, G.; Costanzi, S.; Lambertucci, C.; Taffi, S.; Vittori, S.; Volpini, R. *Farmaco* **2003**, 58, 193.
- Costanzi, S.; Lambertucci, C.; Vittori, S.; Volpini, R.; Cristalli, G. *J. Mol. Graph. Model.* **2003**, 21, 253.
- Gao, Z. G.; Chen, A.; Barak, D.; Kim, S. K.; Müller, C. E.; Jacobson, K. A. *J. Biol. Chem.* **2002**, 277, 19056.
- Gao, Z. G.; Kim, S. K.; Biadatti, T.; Chen, W.; Lee, K.; Barak, D.; Kim, S. G.; Johnson, C. R.; Jacobson, K. A. *J. Med. Chem.* **2002**, 45, 4471.
- Shadnia, H.; Wright, J. S.; Anderson, J. M. *J. Comput. Aided Mol. Des.* **2009**, 23, 185.
- Molecular Operating Environment; C.C.G., Inc., 1255 University St., Suite 1600, Montreal, Quebec, Canada, H3B 3X3.
- Mohamadi, F.; Richards, N. G. J.; Guida, W. C.; Liskamp, R.; Lipton, M.; Caufield, C.; Chang, G.; Hendrickson, T.; Still, W. C. *J. Comput. Chem.* **1990**, 11, 440.
- Cornell, W. D.; Cieplak, P.; Bayly, C. I.; Gould, I. R.; Merz, K. M.; Ferguson, D. M.; Spellmeyer, D. C.; Fox, T.; Caldwell, J. W.; Kollman, P. A. *J. Am. Chem. Soc.* **1995**, 117, 5179.